

# Self-consistent modelling of our Galaxy with Gaia data

James Binney

Rudolf Peierls Centre for Theoretical Physics, University of Oxford, 1 Keble Road, Oxford  
OX1 3NP, UK  
email: binney@thphys.ox.ac.uk

**Abstract.** Galaxy models are fundamental to exploiting surveys of our Galaxy. There is now a significant body of work on axisymmetric models. A model can be defined by giving the DF of each major class of stars and of dark matter. Then the self-consistent gravitational potential is determined. Other modelling techniques are briefly considered before an overview of some early work on non-axisymmetric models.

**Keywords.** stellar dynamics, Galaxy: kinematics and dynamics, (cosmology:) dark matter.

---

## 1. The Standard Galaxy

In 2027 our understanding of the Galaxy will be encapsulated in a software tool that I'll call the Standard Galaxy (SG). The SG, like a Wiki page, will always be a work in progress. When a survey is planned, the SG will be used to simulate the survey's contents in light of its selection function (SF). When the survey is completed, the SG will be updated by maximising the likelihood of the new data with respect to the SG's parameters and the priors from earlier surveys. The SG will describe what's actually out there, which each survey sees only partially.

### 1.1. *What's in the SG?*

- The SG will model the distribution in  $(\mathbf{x}, \mathbf{v})$  of many types of stars:
  - O, B, A, F, G K, M dwarfs, Cepheid variables, RR Lyrae stars, BHB stars, red clump stars, white dwarfs, neutron stars, . . .
  - Most stellar types will be subdivided by age,  $[\text{Fe}/\text{H}]$  and  $[\alpha/\text{Fe}]$  and some will be subdivided by other abundance ratios.
- The SG will also specify the distribution in  $(\mathbf{x}, \mathbf{v})$  of dark matter (DM).
- The SG will include 3-dimensional models of HI, H<sub>2</sub>, the density of H<sup>+</sup> and possibly other chemical species. It will include a model of the interstellar velocity field,  $\mathbf{v}(\mathbf{x})$ .

### 1.2. *The SG and Jeans' theorem*

DM plays an essential role in Galactic structure. But we cannot (yet) actually see it, and there is no guarantee that DM particles will have been detected by 2027. Indeed, even if current efforts to detect DM particles underground bear fruit, measurements of their density and velocity distribution on Earth will add only moderately to what we have already discovered about DM by modelling its contribution to the Galaxy's gravitational field.

The process by which we currently constrain DM by modelling its gravitational field is completely reliant on the assumption that the Galaxy is close to statistical equilibrium. If we drop the assumption that the Galaxy looked pretty much the same 200 Myr ago, and will look essentially the same 200 Myr hence, we can infer nothing about the Galaxy's

gravitational field from the kinematics of stars and gas, because without this assumption of statistical equilibrium any current distribution of matter in phase space is consistent with any gravitational field.

From our reliance on statistical equilibrium to track  $\sim 95\%$  of the Galaxy’s mass, it follows that the foundations of the SG will rest on an equilibrium model of the Galaxy. In reality, the Galaxy is not in equilibrium, even in the rotating frame of the bar, because the stellar halo hosts tidal streams and the disc displays ephemeral spiral arms and a warp. These non-stationary phenomena play key roles in the Galaxy’s evolution (e.g. Aumer & Binney 2017) and promise to be valuable probes of the Galaxy’s assembly history (e.g. Erkal et al. 2016), but they must be excluded from the basic model, which will inevitably be an equilibrium model. Only after its construction will it be decorated with spiral arms, warps and streams.

The natural way to construct an equilibrium model is to exploit Jeans’ theorem: the distribution function (DF) of an equilibrium stellar system may be presumed to depend on  $(\mathbf{x}, \mathbf{v})$  through the constants of stellar motion  $I_1(\mathbf{x}, \mathbf{v}), I_2(\mathbf{x}, \mathbf{v}), \dots$ . Since any function of constants of motion is itself a constant of motion, we have infinite freedom in the choice of the constants of motion that we use as arguments of the DF  $f(\mathbf{I})$ . There is, however, only one rational choice: the action integrals  $J_i$  (e.g. Binney & McMillan 2016). Until recently the use of angle-action variables in galactic dynamics was very limited because we lacked effective ways to convert action-angle coordinates to and from conventional phase-space coordinates. Several numerical schemes for making these transformations are now available (Sanders & Binney 2016). The “Stäckel Fudge” (Binney 2012a) provides the most widely used mapping from  $(\mathbf{x}, \mathbf{v})$  to  $(\boldsymbol{\theta}, \mathbf{J})$  while Torus Mapping (Binney & McMillan 2016) provides the best inverse map. In particular cases the existing tools do have limitations, so further work is required in this area.

### 1.3. *How to assemble a model*

First for each component one wishes to consider, one chooses either a fixed density distribution  $\rho(\mathbf{x})$  or a DF  $f(\mathbf{J})$ . The normalisation of either  $\rho$  or  $f$  is adjusted to ensure that the component’s mass is reasonable. Then one makes a guess at the gravitational potential  $\Phi(\mathbf{x})$  of the final model, and using this potential, the Stäckel Fudge and the DFs one evaluates the model’s density by integrating over velocities at each point of a suitable spatial grid. Then one computes the resulting potential  $\Phi(\mathbf{x})$  and uses this potential instead of the originally guessed potential to re-compute the density at the grid points. This cycle of computing the density using one potential and from it deriving a new potential converges after 4 to 5 iterations (Binney 2014). From this potential and the DFs one can predict *any* observable. The parameters in each component’s DF are adjusted to optimise the fit between the model and observational data (Binney & Piffl 2015).

Given the long tradition of including energy  $E = \frac{1}{2}v^2 + \Phi$  in the arguments of the DF, it’s worth noting that model construction proceeds smoothly as just described only if  $E$  is excluded from the arguments of  $f$ . When  $E$  is included it’s hard to converge on the correct potential, and harder still to ensure that each component has an observationally motivated mass.

### 1.4. *Choice of DFs*

It turns out that simple analytic functions  $f(\mathbf{J})$  generate models that closely resemble familiar models that are defined by simple functional forms of the density  $\rho(\mathbf{x})$ . The isochrone sphere can be exactly generated from an analytic  $f(\mathbf{J})$  (Binney 2014). Posti et al. (2015) showed that the Hernquist, Jaffe and NFW (Navarro, Fren & White 1997)

spheres can be generated to high precision by simple analytic functions  $f(\mathbf{J})$ . Jeffreson et al. (2017) have given an analytic  $f(\mathbf{J})$  which generates a good approximation to a Plummer model. By tweaking the given forms of  $f(\mathbf{J})$ , a spherical model can be endowed with either tangential or radial anisotropy, and it can be flattened or made prolate by the anisotropy (Binney 2014; Binney & Piffl 2015).

It is useful to break the DF into a parts  $f_+(\mathbf{J})$  and  $f_-(\mathbf{J})$  that are even and odd in  $J_\phi$ , respectively. The part  $f_-$  does not contribute to the density but instead controls the model’s rotation. Consequently, a model’s rotation can be readily adjusted to match observational data after its density distribution has been perfected.

Binney & McMillan (2011) introduced the “quasi-isothermal” DF for discs:

$$f_+(\mathbf{J}) = \frac{\Sigma_0 \Omega}{\kappa^2} \exp(-R_c/R_d) \frac{\exp(-\kappa J_r/\sigma_r^2) \exp(-\nu J_z/\sigma_z^2)}{\sigma_r^2 \kappa^{-1} \sigma_z^2 \nu^{-1}}$$

as the simplest DF that creates a plausible disc. Here  $\Sigma_0$  and  $R_d$  are constants that, respectively, set the disc’s mass and approximate scale length, while  $R_c, \Omega, \kappa, \nu, \sigma_r$  and  $\sigma_z$  are all functions of  $J_\phi$ . Specifically,  $R_c, \Omega, \kappa$  and  $\nu$  should be the radius, angular velocity, in-plane and vertical epicycle frequencies of a circular orbit of angular momentum  $J_\phi$  in some potential that is similar to that of the Galaxy. The velocity-dispersion parameters  $\sigma$  should be decreasing functions of  $J_\phi$  and the normal hypothesis is

$$\sigma_i = \sigma_{i0} \exp\left[-\frac{R_c - R_0}{R_{\sigma_i}}\right]$$

where  $\sigma_{i0}$  is a constant that sets the  $i$ th velocity dispersion at the Sun and  $R_{\sigma_i}$  is a constant that determines how rapidly  $\langle v_i^2 \rangle$  declines with distance from the Galactic centre. In a realistic Galactic potential the quasi-isothermal DF produces a disc with an approximately exponential surface density  $\Sigma(R) \simeq \Sigma_0 e^{-R/R_d}$  and a vertical density profile that is sub-exponential in the sense that  $|\mathrm{d} \log \rho / \mathrm{d} z|$  is a slowly increasing function of distance  $z$  from the plane. However, a vertical density profile in which  $|\mathrm{d} \log \rho / \mathrm{d} z|$  decreases with  $z$  as is observed (Gilmore & Reid 1983; Juric et al. 2008) emerges naturally when one models the observed secular increase in  $\langle v_z^2 \rangle$  with age  $\tau$  by modelling each coeval population of stars by a quasi-isothermal with, for example

$$\sigma_{i0}(\tau) = \sigma_{i*} \left( \frac{\tau + \tau_1}{\tau_m + \tau_1} \right)^\beta,$$

where  $\sigma_{i*}$  and  $\tau_m$  are the velocity dispersion and age of the oldest disc stars,  $\sigma_1$  determines the velocity dispersion of these stars at birth and  $\beta \sim 0.5$  controls how the velocity dispersion increases with age.

To date  $f_-$  has been taken to be

$$f_-(\mathbf{J}) = \tanh(J_\phi/J_0) f_+(\mathbf{J}),$$

where  $J_0$  is a constant. This ansatz eliminates counter-rotating stars at angular momenta significantly larger than  $J_0$ , which is assumed to be much smaller than  $R_0 v_c(R_0)$ .

## 2. What’s been done so far

Several papers have fitted models based on DFs  $f(\mathbf{J})$  to data by evaluating moments of the DF in an assumed gravitational potential  $\Phi(\mathbf{x})$ . Adopting a plausible  $\Phi(\mathbf{x})$  rather than solving for the self-consistent potential saves a great many CPU cycles because it is then necessary to compute moments only at locations for which we have data, rather than

throughout the vast extent of the Galaxy (which extends out to  $> 100$  kpc). Moreover, with  $\Phi(\mathbf{x})$  assumed, we only need the moments of components for which we have data. In particular, we don't need to compute moments for the Galaxy's principal component, dark matter.

Binney (2010) fitted a disc DF to data from the Geneva-Copenhagen survey (GCS) (Nordström et al, 2004; Holmberg et al. 2007). The most significant finding of this paper was that the Sun's peculiar velocity  $V_{\odot}$  needed to be revised upwards from  $5.2 \text{ km s}^{-1}$  to  $\sim 11 \text{ km s}^{-1}$ . Schönrich et al. (2010) explained how the standard extraction of  $V_{\odot}$  from the Hipparcos data had been undermined by the metallicity gradient in the disc. Binney (2012b) upgraded his earlier work by using an improved the quasi-isothermal DF (hereafter the "2012 DF") and the just introduced Stäckel Fudge rather than the adiabatic approximation to compute actions. Binney et al. (2014) showed that the 2012 DF had great success in predicting the data from the RAVE survey, which reaches distances in excess of 2 kpc whereas the GCS is essentially confined to distances  $< 0.1$  kpc. The extent to which the 2012 DF captures the strong non-Gaussianity of the velocity distributions in  $v_{\phi}$  and  $v_z$  is remarkable.

Sanders & Binney (2015) proposed an extended DF (EDF) in which  $[\text{Fe}/\text{H}]$  appears alongside  $\mathbf{J}$  as an argument. Since stellar age already appeared in the 2012 DF as a nuisance parameter, with  $[\text{Fe}/\text{H}]$  added to the argument list it became possible to employ stellar isochrones to compute the probability that a star in the model would be included in a given survey. Hence Sanders & Binney (2015) were able to take properly into account survey SFs, which Binney (2012b) and Binney et al. (2014) had neglected to do. They showed that when the SF of the GCS is taken into account, significantly larger values of  $\sigma_{i*}$  are required because the GCS is strongly biased towards young stars, so the stars picked up in the survey have atypically small random velocities.

By fitting an EDF to a sample of SDSS K giants Das & Binney (2016) found evidence for two subpopulations. The EDF Das et al. (2016) fitted to BHB stars showed the older stars to be more tightly confined in action space than the younger stars. Binney & Wong (2017) explored DFs for the Galaxy's disc and halo globular clusters. This exercise revealed that a featureless DF  $f(\mathbf{J})$  is liable to generate a density distribution  $\rho(\mathbf{x})$  on which the gravitational potential has imprinted a feature associated with its transition around  $r \sim 10$  kpc from disc- to halo-domination.

The moments yielded by a given DF depend on the adopted potential  $\Phi$ . Consequently,  $\Phi$  can be constrained by fitting to data the real-space and velocity-space distributions obtained by a particular pair  $(\Phi, f)$ . Bovy & Rix (2013) computed the likelihoods of 43 groups of stars over a 5-dimensional grid in  $(\Phi, f)$  space. Each stellar group comprised the  $\sim 400$  G dwarfs from the SEGUE survey that lie in a cell in the  $([\text{Fe}/\text{H}], [\alpha/\text{Fe}])$  plane. The DF was constrained to be a quasi-isothermal and  $\Phi$  was generated by a spherical bulge and dark halo plus double-exponential stellar and gas discs. The bulge was a fixed Hernquist model and the dark halo was a power-law model, so its free parameters were its logarithmic slope and its local density. The mass and scale lengths of the stellar disc were free parameters. The likelihood of each stellar group was computed over a 5-dimensional grid in  $(\Phi, f)$  space. Unfortunately, the likelihood distributions in  $(\Phi, f)$  space of the different populations were not mutually consistent. This is not surprising since the phase-space distribution of stars of a given chemical composition cannot be well modelled by a quasi-isothermal. In particular, stars with low  $[\alpha/\text{Fe}]$  and low  $[\text{Fe}/\text{H}]$ , being relatively young low-metallicity stars, have to be confined to an annulus centred beyond  $R_0$ .

Piffl et al. (2014) took a different approach to choosing a  $(\Phi, f)$  pair, and they exploited the kinematics of  $\sim 200\,000$  giant stars from the RAVE survey rather than  $\sim 17\,000$

SEGUE stars. They computed a  $\chi^2$  statistic for the fit provided by  $(\Phi, f)$  to both the RAVE kinematics and the density of stars  $\rho(z)$  extracted from SDSS star counts by Juric et al. (2008) and two diagnostics of the Galaxy’s circular-speed curve: terminal velocities measured from CO and HI data, and astrometry of maser sources. They homed in on the best  $(\Phi, f)$  pair by first adopting a local dark-halo density  $\rho_{\text{DM}}$ , finding the disc that then best reproduces the diagnostics of the circular speed and the kinematics of RAVE giants and then computing the resulting vertical density profile of the disc. If the initially assumed  $\rho_{\text{DM}}$  is small, a massive disc is required to match constraints on the rotation curve, and then given the RAVE kinematics the disc is too thin to match the SDSS  $\rho(z)$ . When  $\rho_{\text{DM}} \simeq (0.013 \pm 0.002) M_{\odot} \text{pc}^{-3}$  all data are fitted quite nicely. The principal uncertainty is the shape of the dark halo: a more oblate dark halo requires a less massive disc to complement it. It turns out that the mass of the dark halo at  $R < R_0$  is almost independent of the halo’s axis ratio.

Piffl et al. (2015) first took the major step of specifying the dark halo by a DF  $f(\mathbf{J})$  rather than a parametrised density distribution. Once this step is taken, it no longer makes sense to use a parametrised potential  $\Phi$  and the model is completely specified through the self-consistency condition by the DFs of its constituent populations. For the disc, Piffl et al. adopted the DF fitted by Piffl et al. (2014), while for the dark halo they chose the DF that would in isolation self-consistently generate the NFW density profile determined by Piffl et al. (2014). When the self-consistent model implied by these two DFs was constructed, its circular-speed curve proved inconsistent with the data at  $r \lesssim 3 \text{ kpc}$  because the dark halo was pulled inwards and towards the plane by the gravitational field of the disc.

Binney & Piffl (2015) took the obvious next step: search the space  $(f_{\text{disc}}, f_{\text{DM}})$  for a pair of DFs that self-consistently generate a model that is consistent with all the data assembled by Piffl et al. (2014). In this search the functional forms of the DFs were the same as those adopted by Piffl et al. (2015) but the parameters were free. A model that satisfied the observational constraints was found. It did however, have a remarkably large disc scale-length (3.7 kpc) and it did not produce as high an optical depth to microlensing bulge stars as microlensing surveys require (Sumi & Penny 2016). The reason for these short-comings was clear: in order to keep the circular speed at  $R \sim 3 \text{ kpc}$  within the observational upper limit, stars had been shifted outwards by increasing  $R_{\text{d}}$ , leaving dark matter, which does not cause microlensing, the dominant mass density at small radii.

This finding establishes a tension between (i) the local density of DM that one deduces from  $v_c(R_0)$  and the kinematics and thickness of the disc, (ii) the assumption that DM has been adiabatically compressed by the gravitational field of slowly inserted baryons, and (iii) the density of stars at  $R \lesssim 3 \text{ kpc}$  required by the microlensing data. The clear next step is to drop the assumption that DM has responded adiabatically to the insertion of baryons.

The NFW density profile implies that  $f_{\text{DM}}$  diverges as  $\mathbf{J} \rightarrow 0$ , because the divergence of  $\rho_{\text{DM}}(r)$  as  $r \rightarrow 0$  is accompanied by decreasing velocity dispersion. This prediction of simulations of cosmological clustering in the absence of baryons must be a consequence of the assumed extremely large density of DM at high redshift. The very high phase-space density of DM at the centre of an NFW halo will be drastically lowered when a passing clump of baryons imparts even a tiny velocity kick to DM particles. Once the phase-space density of DM has been reduced in this way, by Liouville’s theorem it cannot be increased. Moreover, the efficient scattering of particles in a confined region of phase space will drive the phase-space density to a constant, which is the state of maximum entropy

subject to constrained mean phase-space density. So Cole & Binney (2017) took the view that a probable  $f_{\text{DM}}(\mathbf{J})$  is one that tends to a constant as  $\mathbf{J} \rightarrow 0$ , where scattering by baryons has been efficient, and tends to the NFW  $f(\mathbf{J})$  at high energies, where scattering has been unimportant. The transition between these two asymptotic regimes must be consistent with conservation of DM by scattering. Cole & Binney (2017) devised a form for  $f_{\text{DM}}(\mathbf{J})$  that is consistent with these principles and successfully searched the space ( $f_{\text{disc}}, f_{\text{DM}}$ ) for models consistent with the P14 data plus the microlensing constraints. Their new  $f_{\text{DM}}(\mathbf{J})$  has an additional parameter  $h_0$ , which specifies the transition between the regime of approximately constant  $f_{\text{DM}}$  and the regime in which  $f_{\text{DM}} \sim f_{\text{NFW}}$ . In the absence of baryons their favoured  $h_0 \sim 150 \text{ kpc km s}^{-1}$  implies a DM core radius  $\sim 3 \text{ kpc}$ , but the dark halo doesn't have a core in presence of the baryons.

Through the sequence of models of increasing sophistication just described, the local density of DM has changed very little from the value  $\rho_{\text{DM}} \simeq 0.013 M_{\odot} \text{ pc}^{-3}$  determined by Piffl et al. (2014).

### 2.1. Models not based on actions

Most models of external galaxies are based either on the Jeans equations or on the technique introduced by Schwarzschild (1979) (Akin et al. 2016). The best current models of the Galactic bar (Portail et al. 2017) use the ‘‘made-to-measure’’ variant of Schwarzschild’s technique (Syer & Tremaine 1996; de Lorenzi et al. 2007). Jeans models certainly lack the rigour and flexibility required to do justice to Galactic data. In Schwarzschild and made-to-measure models the initial conditions of numerically integrated orbits play the role of constants of motion and weights assigned to orbits play the role of the value taken by the DF on an orbit. It is relatively simple to fit such models to observational data, and neither deviations from axisymmetry nor resonant trapping are problematic. The major differences with  $f(\mathbf{J})$  modelling are (i) the DFs have vastly more parameters than a typical  $f(\mathbf{J})$ , and (ii) the orbit labels they use are complex and devoid of physical meaning.

I see several reasons why these models are unlikely to rise to the challenge posed by data in the era of Gaia. First, such a model is cumbersome because it is specified by millions of weights with low individual information content. Consequently, it’s hard to compare models – two models with identical physical content will have no two parameters the same because each model will sample phase space in a different way. Moreover, the lack of a systematic scheme for labelling orbits that’s invariant under changes in the gravitational potential means that it’s hard to refine a model by subdividing components into sub-groups. For example, as data on the age distributions of giants accumulate, one will want to subdivide stars on the giant branch into age cohorts. Such refinements will invariably be associated with a change in the self-consistent potential and it’s important to be able to identify orbits before and after such a change.

An additional issue with models of the Schwarzschild type is that it is difficult to include DM in the modelling process. One issue is that the quantity and spatial extent of DM necessitates a huge increase in the particle count. A more profound issue is that *no* observational data directly constrain DM – all constraints come indirectly through observational constraints on visible matter. It is not clear that current techniques can assign weights to DM particles.

It will never be possible to fit a standard N-body model to the exquisite data for our Galaxy, but generic N-body models have a huge role to play because they uniquely enable us to model from first principles evolutionary processes such as secular heating and radial migration (e.g. Aumer et al. 2016; Aumer & Binney 2017).

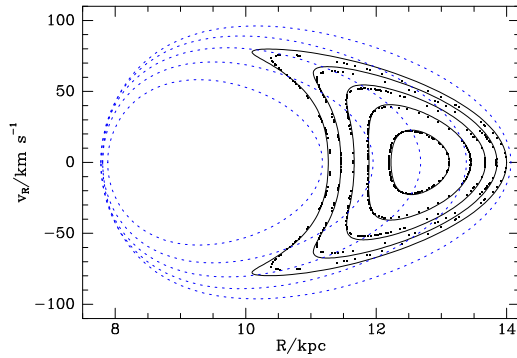


**Figure 1.** A surface of section  $\phi = z = 0$  in a realistic barred Galaxy model. The full black curves are perturbatively constructed cross sections through tori trapped by the bar’s OLR. The points are consequents on orbits started from a point on each of these curves. The dashed blue curves show cross sections through the underlying axisymmetric tori.

### 3. What next?

Not only is our Galaxy barred, but numerical simulations of the secular growth of a disc within a dark halo show that spontaneously generated, transient non-axisymmetries account very naturally for the structure of the thin disc (Aumer et al. 2016; Aumer & Binney 2017). Moreover, it now seems likely that the bar’s corotation resonance lies as far out as  $R \simeq 6$  kpc, so the kinematics of solar-neighbourhood stars are significantly affected by the bar. Hence it is essential to regard axisymmetric models as spring-boards from which to progress to models that include both a bar and spiral structure.

As noted above, angle-action variables provide the natural arena for perturbation theory, and a major attraction of models built around analytic DFs  $f(\mathbf{J})$  is the ease with which we can perturb them. The impact of a perturbing potential  $\Phi_1(\boldsymbol{\theta}, \mathbf{J})$  on a model with DF  $f(\mathbf{J})$  can be computed by linearising the Boltzmann equation:  $f_0(\mathbf{J}) \rightarrow f_0(\mathbf{J}) + f_1(\boldsymbol{\theta}, \mathbf{J}, t)$ . With  $[a, b]$  denoting the Poisson bracket, we have

$$\frac{\partial f_1}{\partial t} + [f_0, \Phi_1] + [f_1, \Phi_0] = 0.$$

This equation is readily solved once one knows the Fourier expansion  $\Phi_1 = \sum_{\mathbf{n}} \phi_{\mathbf{n}}(\mathbf{J}) e^{i\mathbf{n} \cdot \boldsymbol{\theta}}$  of the perturbing potential. Monari et al. (2016) have used this approach to compute the response of thin-disc stars at the bar’s outer Lindblad resonance (OLR), which Dehnen (2000) argued lies just beyond  $R_0$ .

Unless  $\Phi_1$  is extremely small, sufficiently near the resonance  $f_1$  becomes larger than  $f_0$ . This is problematic because the sign of  $f_1$  fluctuates, so once  $f_1$  exceeds  $f_0$  the total DF  $f_0 + f_1$  is liable to be negative, which is unphysical.

The linearised Boltzmann equation breaks down when orbits become trapped by a resonance. Far from a resonance, the phase-space tori to which stars on regular orbits are confined are merely distorted by  $\Phi_1$ . At a critical distance from the resonance, the tori abruptly rearrange themselves into a completely new pattern, and we say that the old tori/orbits have been trapped by the resonance. Angle-action variables enable us to reduce this phenomenon to a one-dimensional problem, closely analogous to the dynamics of a pendulum. Untrapped orbits correspond to a pendulum that rotates fast enough to pass top dead-centre and rotate always in the same sense, while trapped orbits correspond to a pendulum that swings to and fro as in a clock. Trapped orbits cannot be characterised by the same set of actions that characterise untrapped orbits, but must be assigned an entirely new “action of libration” in addition to two linear combinations of the original

actions (e.g. Binney 2016). Consequently, for each family of resonantly trapped orbits we require a new DF  $f(\mathbf{J})$  in addition to the familiar DF of the untrapped orbits.

Fig. 1 shows that when one uses the angle-action coordinates that torus mapping provides and the enhanced pendulum equation that Kaasalainen (1994) introduced, one can obtain remarkably accurate analytic models of trapped orbits. Specifically the figure shows a surface of section  $(R, v_R)$  at  $\phi = 0, z = 0$  for motion in a realistic barred Galactic potential. The full curves are cross sections through tori trapped by the OLR of a realistic barred Galaxy model. These curves agree extremely well with the lines of dots, which are consequents of orbits integrated from an initial condition provided by one point on each curve. The blue dashed curves are cross sections through the axisymmetric tori that underpin the perturbative results.

## References

- Akin, Y., et al., 2016, 456, 538  
 Aumer, M., Binney, J. & Schönrich, R., 2016, MNRAS, 459, 3326  
 Aumer, M. & Binney, J., 2017, MNRAS accepted (arXiv1705.09240)  
 Erkal, D., Belokurov, V, Bovy, J. & Sanders, J.L., 2016, MNRAS, 457, 3817  
 Arnold, V.I., 1978, *Mathematical methods of classical mechanics*, Berlin: Springer  
 Binney, J., 2010, MNRAS, 401, 2318  
 Binney, J., 2012a, MNRAS, 426, 1324  
 Binney, J., 2012b, MNRAS, 426, 1328  
 Binney, J., 2014, MNRAS, 440, 787  
 Binney, J., 2016, MNRAS, 462, 2792  
 Binney, J., Burnett, et al., 2014, MNRAS, 439, 1231  
 Binney, J. & McMillan, P.J., 2011, MNRAS, 413, 1889  
 Binney, J. & McMillan, P.J., 2016, MNRAS 456, 1982  
 Binney, J. & Piffl, T., 2015, MNRAS, 454, 3653  
 Binney, J & Wong, L.K., 2017, MNRAS, 467, 2446  
 Das, P. & Binney, J., 2016, MNRAS, 460, 1725  
 Das, P., Williams, A. & Binney, J., 2016, MNRAS, 463, 3169  
 Bovy, J. & Rix, H.-W., 2013, ApJ, 779, 115  
 Cole, D. & Binney, J., 2017, MNRAS, 465, 798  
 Dehnen, W., 2000, AJ, 119, 800  
 de Lorenzi, F., Debattista, V.P., Gerhard, O. & Sambhus, N., 2007, MNRAS, 376, 71  
 Gilmore, G. & Reid, N., 1983, MNRAS, 202, 1025  
 Holmberg, J, Nordström, B. & Anderson, J., 2007, A&A, 475, 519  
 Jeffreson, S.M.R., 14 others 2017, MNRAS, submitted  
 Juric, M. et al., 2008, ApJ, 673, 864  
 Kaasalainen, M., 1994, MNRAS, 268, 1041  
 Monari, G., Famaey, B., Siebert, A., 2016, MNRAS, 457, 2569  
 Navarro, J., Frenk, C.S. & White, S.D.M., 1997, ApJ, 490, 493  
 Nordström, B. et al., 2004, A&A, 418, 989  
 Piffl, T. et al., 2014, MNRAS, 445, 3133  
 Piffl, T., Penoyre, Z. & Binney, J., 2015, MNRAS, 451, 639  
 Portail, M., Gerhard, O., Wegg, C & Ness, M., 2017, MNRAS, 465, 1621  
 Posti, L., Binney, J., Nipoti, C. & Ciotti, L., 2015, MNRAS, 447, 3060  
 Sanders, J.L., & Binney, J., 2015, MNRAS, 447, 2479  
 Sanders, J.L. & Binney, J., 2016, MNRAS, 457, 2107  
 Schönrich, R., Binney, J., Dehnen, W., 2010, MNRAS, 403, 1829  
 Schwarzschild, M., 1979, ApJ, 232, 236  
 Sumi, T. & Penny, M.T., 2016, ApJ, 827, 139  
 Syer, D. & Tremaine, S., 1996, MNRAS, 282, 223